ANALYSIS AND PERFORMANCE EVALUATION OF ANFIS CONTROLLED RESONANT CONVERTER

SOUNDIRARAJ NALLASAMY[1], RAJASEKARAN VAIRAMANI[2]
[1] Assistant professor,[2] Professor,
Department of Electrical and Electronics Engineering, PSNA College of Engineering and Technology, Dindigul, Tamilnadu-624622,soundar06@gmail.com

Abstract *--- This article presents the dynamic, stability analysis and frequency reaction of LLC resonant converter (LLC RC) and also three control methods developed and implemented both simulation and experimentally. The control and stabilization of LLC resonant converters are major problems in power electronics. The modeling of the LLC resonant converter is originated by employing the describing function approach and then, proportional integral and derivative (PID), Spectator and Adaptive Neuro-fuzzy inference system (ANFIS) controllers are designed and developed. The above said controllers simulated using MATLAB and experimentally implemented with Texas instruments piccolo TMS320F28069 DSP microcontroller. Design, simulation, and investigational results for a 200 voltage, 7.5 ampere, 1.5 kW and 106 kHz LLC RC are presented in this paper. The ANFIS controller provides better voltage regulation, better efficiency and capable to stabilize the output effectively even under unexpected deviation of load.*

Key Terms*—DC/DC resonant power conversion, nonlinear systems, stability analysis, transient response, frequency response, ANFIS controller, spectator controller, PID controller.*

1.Introduction

In last few years, the plan and improvement of a variety of resonant converters have been paying attention on communication and space research applications. Then it is observed that those converters have maximum switching victims, minimum reliability, interference, and acoustical noise at maximum frequencies. Those resonant converters were classified into two basic topologies such as series resonant converters and parallel resonant converters which have two reactive elements. Because of several inherent benefits a series-parallel resonant converter (SPRC) is discovered to be desirable. In SRC the capacitors are connected in a serial manner and the isolation transformers possess inherent DC blocking capability so that it can provide better load efficiency. Nevertheless, it has poor load regulation and at no load condition switching frequency is varied so that the output voltage regulation is not possible. But then, the PRC provides improved no-load regulation and it has insufficient load regulation because of the deficiency of DC blocking at the isolation transformer. In order to attain better voltage regulation an RC is combined with three reactive components. Control and power circuits have been embedded in a single chip in various integrated circuits to minimize the design causes and also to reduce component parameters like dimension, cost and count of LLC DC/DC converters [1]. Unique power devices and experienced control stages are required by High-power applications (kW) which are implemented in field programmable gate Arrays or dedicated microprocessors [2]. The operation of parallel circuit is simple and it does not require any complicated control circuit that raises the ripple frequency. There are so many Fuzzy Logic Controllers (FLCs) for DC–DC converters [3] – [5] have presented and implemented. Those controllers have proven assurance in handling with non-linear control systems and attaining voltage regulation at buck converters. Those controllers had proven assurance in handling with nonlinear control systems and attaining voltage regulation in buck converters. To show the dynamics of non-linear system FCL requires human-like semantic phrases in the formation of IF–THEN rules. Qiu et al. [6] have presented various FLC techniques that depend on the human power to realize the performance of the system which follows qualitative control rules. Most of the DC–DC Converters are comprised of FLC technique with same control rules. Nevertheless, based on the converter parameters and topology some scale factors have to be tuned and by using buck-boost converter the proposed technique is tested and presented. Tschirhart and Jain [7] proposed a DC/AC SRC with constant load measure regarding two control techniques. Sivakumaran and Natarajan [8] introduced a CLC SPRC employing FLC for load as well line regulation. Through the evaluated controller performance it can be observed that the independent operation of load might not be feasible. Borage et al. [9] have proposed a FLC based zero voltage switching quasi-RC in which the load independent operation is not accomplished and it has very poor power handling capability. Guo et al [10] presented a DSP-based PID and fuzzy controllers for dc–dc converters and it is discovered which under various load conditions, the fuzzy controller produced less oscillation. When the load is decreased the peak

changes is higher. Beiranvand et al [11] have analyzed a wide-adjustable-range LLC RC. Then, the implementation of digital controllers for resonant controllers is presented by Yepes et al [12] which uses two integrators. Hong et al. [13] have presented the design of cost efficient secondary-side LLC resonant controller IC for an LED back light units. Beiranvand et al. [14] have demonstrated the design and analysis of an LLC RC which has a broad range of output voltage. Feng et al. [15] proposed a universal adaptive SR driving approach for LLC RCs. Anthony et al. [16] have introduced a universal design for a non-isolated resonant gate driver circuit. While considering the power electronics circuits, circuit averaging and state-space averaging (SSA) approaches are the most popular techniques in circuit modeling, but when the switching frequency is higher than the circuit frequency, the circuit becomes unreliable [17]. AC signal variation must be substantially lower than its quiescent operating levels that are not fulfilled in resonant converters. If switching frequency harmonics present in inductor and magnetizing current, capacitor and primary transformer voltage, there should be a non-linear coupling exist between Alternate Current (AC) and Direct Current (DC) state variables. Furthermore, the natural frequency is near to the resonant circuit's switching frequency. Thus, in LLC resonant converter modeling, circuit averaging and SSA approaches cannot be employed [18], [19]. In this study, Describing Function (DF) method [20], [21], [22], based first harmonic sinusoidal approximation state variables are taken to derive exact small and large signal models of the LLC resonant converter. The non-linear system possesses dynamic behavior which is obtained to replace every non-linear element by descriptive function. There is a relationship between descriptive function and input amplitude that the gain of descriptive function is a function of the circuit's input amplitude. Therefore, input and modulating function sets are developed in which the modulating functions relate the state and the control variables [22]. Frequency controlled resonant converter is proposed; however, a design for the phase modulation is also attained. A Luenberger is a type of observer which renders for state variable approximation [23]. Park et al. [24] have presented an enhanced switching technique of non-isolated step-up DC–DC converters. Lee and Moon [25] demonstrated an analysis of state trajectory that is employed to discover ideal design of converter parameters. Sano and Fujita have described a control technique of SCRC with its soft-switching function. LLC resonant converters are widely adopted as a front-end converter in distributed power system for the telecommunication, computer and network applications . This paper presents the model of the LLC resonant converter which was formulated by employing the describing function approach, then, proportional integral and derivative (PID), Spectator and Adaptive Neuro-fuzzy inference system (ANFIS) controllers were designed and developed. The above said controllers simulated using MATLAB and experimentally implemented with Texas instruments piccolo TMS320F28069 DSP microcontroller. Design, simulation, and experimental results for a 200 voltage, 7.5 ampere, 1.5 kW and 106 kHz LLC RC are presented. The ANFIS controller provides better voltage regulation, better efficiency and capable to stabilize the output effectively even under sudden variation of load. The remainder of the paper is organized as follows: section II addresses non linear model and design based on describing function of LLC RC .Section III describes stability analysis of LLC RC.Section IV deals design of the PID, spectator and design of ANFIS controllers. Section V demonstrates and analyzes the acquired experimental results, finally, Section VI comprises the conclusions.

2.Nonlinear Design Of LLC Resonant Converter

As depicted in Figure. 1, the LLC resonant converter possesses four passive elements; the resonant tank comprises three elements and remaining at the output filter. In order to drive a mathematical theory using a sinusoidal approximation, the resonant tank is fragmented into sine and cosine elements. Through this result LLC resonant converter's nonlinear model can be obtained.

Model Development

By using the Kirchhoff's current and voltage laws to Figure 2,the equations (1) – (4) can be found easily

$$\frac{di_r}{dt} = \frac{1}{L_s}V_{in} - \frac{T_s}{L_s}i_r - \frac{1}{L_S}V_C - \frac{n}{L_s}sign(i_r - i_m)V_{cf} \quad (1)$$

$$\frac{dV_c}{dt} = \frac{1}{C_s}i_r \quad (2)$$

$$\frac{di_m}{dt} = \frac{n}{L_m}V_{cf}sign(i_r - i_m) \quad (3)$$

$$\frac{dV_c}{dt} = \frac{n}{C_f}|i_r - i_m| - \frac{1}{R}V_{cf} \quad (4)$$

Where V_{in} is a voltage of square wave produced by the full bridge switches which is the input of the resonant tank circuit and i_r, V_C , i_m and V_{cf} are the state variables.

Harmonic Estimation

When applying the sinusoidal estimation, the AC state variables such as i_r , V_C , and i_m (in (1)–(4)) are fragmented into sine and cosine elements. In order to get steady state measures, the derivatives are equalized to zero. However, this fragmentation generates two different classes for every ac variable and extends to seventh order dynamic design. Series resonant current estimation is shown in eqn (9) and (10)

$$i_r(t) = i_{rs}(t)sin(\omega_s t) - i_{rs}(t)cos(\omega_s t) \quad (9)$$

$$\frac{di_r}{dt} = \left(\frac{di_{rs}}{dt} + \omega_s i_{rc}\right)sin(\omega_s t) - \left(\frac{di_{rc}}{dt} + \omega_s i_{rs}\right)cos(\omega_s t) \quad (10)$$

From the equation (9) and (10), it is observed that the output voltage is independent of the load resistance. Also the converter gain adopts a sine function. To sustain the output voltage at fixed rate of suitable measure with the fluctuations at the load

resistance and supply voltage, the output pulse width must be switched in a closed loop manner. Nevertheless, the expected variation in pulse width is actually small.

C. Describing Function (DF)

The concept of DF is one of the most powerful tools in mathematical field for designing resonant $F_1(d, V_{in}), F_2(i_s, i_p, i_{cf}), F_3(i_s, i_p, v_{cf})$ and $F_4(i_s, i_c)$.

$$F_1(d, V_{in}) = \frac{4V_{dc}}{\pi} sin(\pi d) = \frac{4V_{dc}}{\pi} \quad (5)$$

$$F_2(i_s, i_p, i_{cf}) = \frac{4}{\pi}\frac{i_s}{i_p} V_{cf} \quad (6)$$

$$F_3(i_s, i_p, v_{cf}) = \frac{4}{\pi}\frac{i_s}{i_p} V_{cf} \quad (7)$$

$$F_4(i_s, i_c) = \frac{2}{\pi} i_p \quad (8)$$

By utilizing eqn (7)–(10), the nonlinear terms of (1)–(4) can be estimated below

$$V_{in}(t) = F_1(d, V_{in}) \sin(\omega, t) \quad (11)$$

$$\sin(i_r - i_m) V_{cf} = F_2(i_s, i_p, v_{cf}) \sin(\omega_s t) - F_3(i_s, i_p, v_{cf}) cos(\omega_s t) \quad (12)$$

converters and examining their dynamic operation [26]. These approaches have both analysis of time and frequency domain and extract the design by dividing modulated waveforms into sine and cosine waveforms. The nonlinear conditions, specified in (1)–(4) can be estimated to their primary harmonic terms. The DFs are outlined as

$$|i_r - i_m| = F_4(i_s, i_c). \quad (13)$$

By using (7)–(13) from (1)–(4), distinguishing the sine terms and cosine terms, the succeeding equations are acquired

$$\frac{di_{rs}}{dt} = \frac{4V_{dc}}{\pi L_s} - \omega_s i_{rc} - \frac{r_s}{L_s} i_{rs} - \frac{1}{L_s} v_{cs} - \frac{4n}{\pi L_s} \frac{i_{rs} - i_{ms}}{i_p} V_{cf} \quad (14)$$

$$\frac{di_{rc}}{dt} = \omega_s i_{rs} - \frac{r_s}{L_s} i_{rc} - \frac{1}{L_s} v_{cc} - \frac{4n}{\pi L_s} \frac{i_{rc} - i_{mc}}{i_p} V_{cf} \quad (15)$$

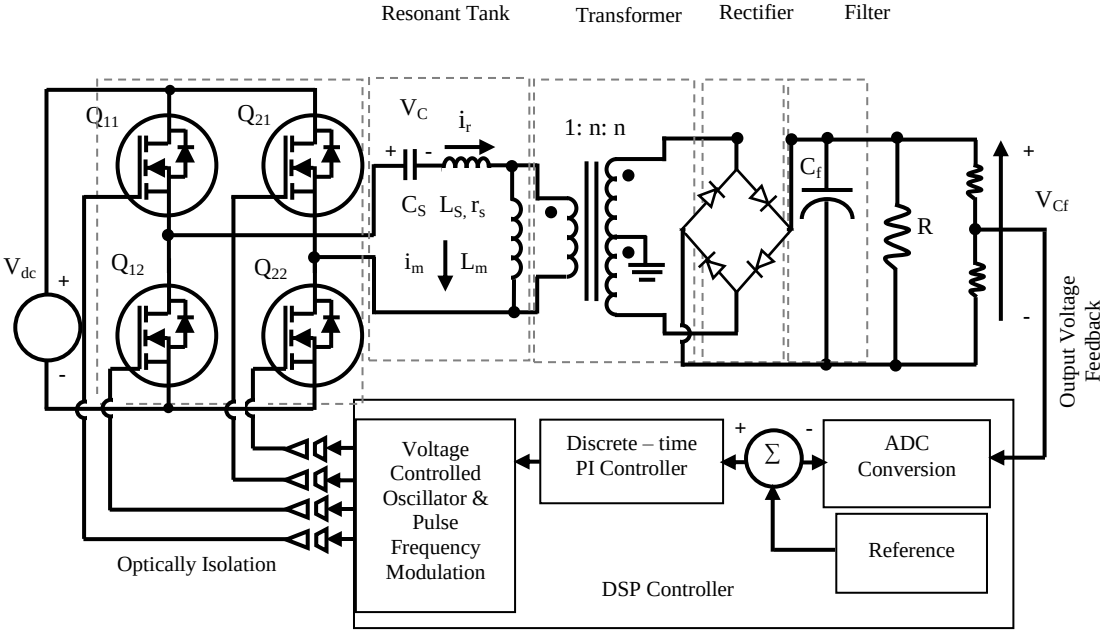

Fig. 1. Schematic diagram of the LLC resonant DC/DC converter

3.Design Of The PID Controller

A PID controller is defined as a three terms controller, and its transfer function is as follows

$$G_c = K_p + K_p T_d s + \frac{K_p}{T_i s} \quad (16)$$

To tune PID controllers there are various prescriptive rules are employed and in our proposed technique the Ziegler-Nichols approach is need to tune the gain measure (kp, Td, and Ti). Some of the applications of dc-to-dc converters generally employed PID based controllers. Fig. 7 shows the block diagram of the converter controlled by PID controller. The integrator term was realized by the Backward Euler method which is otherwise called as Backward Rectangular or Right-Hand approximation. Accordingly, approximation is done at the integrator and the output expressions of the PID controller up to step n are given below:

$$u(n) = u(n-1) + \left(K_p + K_1 T_s + K_D/T_s\right) e(n) + \left(-K_p - 2\,K_D/T_s\right) e(n-1) + K_D/T_s\, e(n-2) \quad (17)$$

where e(n) and u(n) represent the error signal and output of the controller at step n, respectively.Ziegler and Nichols [29] conducted numerous experiments and proposed rules for determining values of K_P ,K_I

and K_D based on the transient step response of a system.

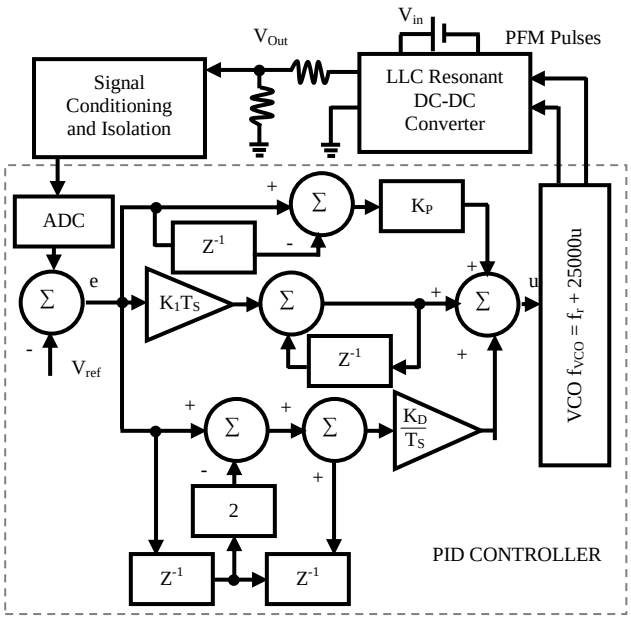

Fig.2 Block diagram of the converter with PID controller

It is applied to a RC with either integrator or dominant complex conjugate poles and its unit step response is similar to an S-shaped curve without any overshoot. The S-shaped curve is otherwise known as the reaction curve which is depicted in Fig.8. The reaction curve is denoted by two major constants such as delay time constant (L) and time constant (T). Both constants were decided by making a tangent line in the curve's inflection point and discovering the overlaps of the tangent line with the time axis and the steady-state level line. By employing the parameters L and T, the measures of K_P , K_I , and K_D are set according to the formula shown in the Table I.

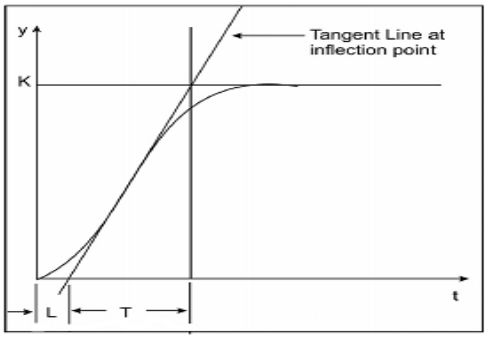

Fig .3.S-shaped reaction curve

TABLE II
Ziegler- Nichols Parameters for PID Controller

Control TYPE	**K_P**	**K_I**	**K_D**
PID	0.6K	$2K_P/T_U$	$K_P\ T_U/8$
	0.09	700	2.9e-6

4. Design Of Spectator Based Controller

A spectator has been build to add a term of feedback at the output error by creating a copy of the master system equations and the condition of eqn (22) is approximated by applying the spectator [31]. The purpose of spectator to deal and control the power electronics devices is already dealt in [32]-[34]. The law of spectator-based control is as follows:

$$\dot{\epsilon}\,(t) = f\big(\varepsilon(t), V_{in}(t), R(t), \omega_s(t)\big) + r\left(V_{cf}(t) - \varepsilon_7(t)\right)$$

$$\omega_s(t) = \dot{\omega}_s(t) - K\big(\varepsilon(t) - \bar{X}\,(t)\big) \tag{18}$$

the controller is implemented by employing a Digital Signal Processor, equations in (34) must be rewritten in discretized form

$$\varepsilon\big((k+1)\Delta\big) = \varepsilon(k\Delta) + r\left(V_{cf}(k\Delta) - \varepsilon_7(k\Delta)\right)$$

$$+\Delta f\big(\varepsilon(k\Delta), V_{in}(k\Delta), R(k\Delta), \omega_s(k\Delta)\big)$$

$$\omega_s(k\Delta) = \dot{\omega}_s(k\Delta) - K\big(\varepsilon(k\Delta) - \bar{X}\,(k\Delta)\big) \tag{19}$$

Implementation

The spectator is initialized by realizing the closed loop system in the steady state measure $\bar{X}$that is accessible in the ongoing load and input voltage, with the help of the design formerly depicted in eqn (22). To compute the eqn (34), the Euler's estimation technique is employed (23). Some other superior technique such as Runge Kutta [35], can be assumed but it requires more computational time. However, it is observed that implementation of spectator controller of eqn (34) in DSP follows easy steps through (35) and still by employing the lookup table which gives better results. By employing eqn (22), switching frequency and steady state measures of state variables for lookup table is computed without conducting any experiments. Likewise, the gain and the approximated feedback are adjusted once which is not varied for different input voltage and load conditions. The controller need to execute the given steps at every sampling time: 1) the ongoing input and output voltages and load are observed; 2) the state variables and switching frequency were recorded by utilizing the lookup table according to the range of ongoing input voltage and load; 3) the control law is computed [i.e., ωs, (kΔ) in (35)], which is to be utilized at the sampling interval through zero-order control; 4) through Euler's estimation the approximated state variables are computed for adjacent sampling time [i.e., ξ ((k + 1)Δ) at (35)]. Here in this paper, the range of input voltage and load has been taken as 5-V steps and 10- Ω steps respectively. The steady state measures of $\bar{\omega}$ and $\bar{X}$ is needed to implement the spectator based controller in eqn (35) at various measures of the input voltage and load as optimum estimated at the lookup table. Control gain K and Gain vector Γ are the following. (36), (37).

$$r = [0.2\ \ 0.2\ \ 0.3\ \ -0.1\ \ -0.25\ \ 0.6\ \ \ 0.8]^T \tag{20}$$

$$K = [2\ \ \ 25\ \ \ 4\ \ \ -0.25\ \ \ -30\ \ \ 6\ \ \ 2] \tag{21}$$

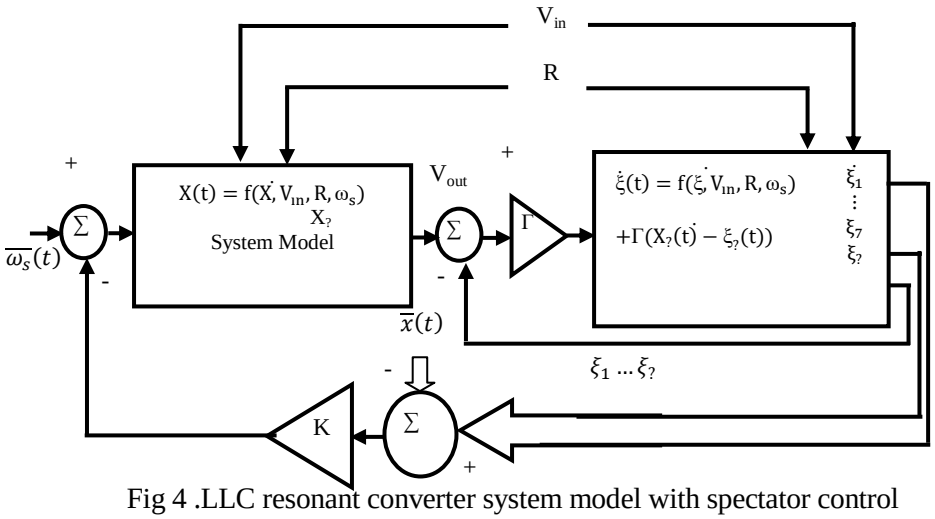

Fig 4 .LLC resonant converter system model with spectator control

5.Design Of An ANFIS Controller

Artificial neural network (ANN) is a type of mathematical example which has the capabilities of learning as well as parallel data processing. This employs computational neurons that are coordinated at layers and linked to one another through weight factors. Then, ANNs possess some of the features such as nonlinear and adaptative structure, observation skills, and design independence of system parameters. Thus it can be employed in microprocessor control systems. But it has less number of rules to define the structure because of its instruction trouble [37], [39] and "black box" nature of the network. In 1993, Jang [36] has presented ANFIS which is the most efficient neuro-fuzzy system that implements neural learning rules in order to discover and adjust the structure and parameters of the fuzzy inference system and it is mainly established on the unused data. Its major features are given in [38]–[39] such as: a) easy implementation; b) powerful generalization skills; c) quick and précised learning skills; d) simple fuzzy rules provides easy understanding e) for problem solving it has easy incorporation of both numeric and linguistic knowledge. Fig. 9 has shown regualr architecture of an ANFIS [35]–[38] where the circle points a constant node and a square suggests an adaptative node. Then a multilayered feed-forward network is demonstrated in which every layer possess a specific operation along the input signal.

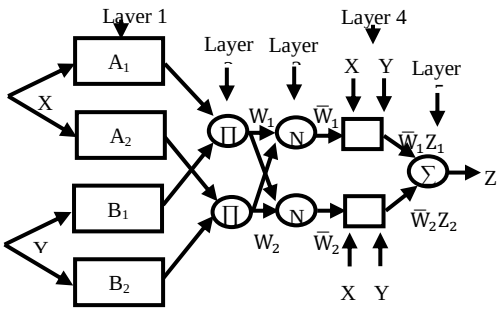

Fig. 5. Typical architecture of ANFIS [35]–[38].

In ANFIS, (x, y) are two inputs and Z is the output which has five layers. At the beginning layer the nodes (A_i , B_I) has the MF allotted to each input (x, y). and at the second layer there are two rules can be identified such as rule 1: x= A_2 and y = B_1 ; rule 2: x= A_2 and y = B_2. The normalized firing strength of every rule (w_1, w_2) is computed at the third layer. The linear functions are included at the fourth layer that is input signal functions. Each rule has the normalized firing strength which is estimated at the precedent layer. At last, the overall performance is computed by the fifth layer by adding all incoming signals. The trained data has the ability to tune the parameters of the Membership function (MF). In this paper, the output of the LLC resonant converter is controlled by the ANFIS which is applied by employing the Fuzzy Logic Toolbox of MATLAB [39]. In order to regularize the output power to load in LLC RC converter an ANFIS based control system is employed. Fig. 10 has demonstrated the voltage and current required by the load.

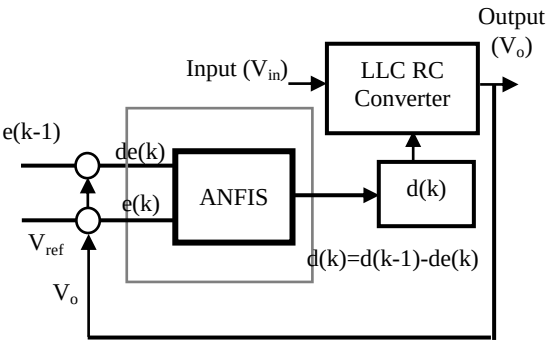

Fig. 10. ANFIS based control system.

To estimate the error "X" the direct RMS measures of the sinusoidal reference and load voltages and variations in error "Y" signals which play as the ANFIS controller's input are needed at each sampling interval. There is 1600 testing and training data are needed to describe the ANFIS controller and these data are chosen from the system simulations under

consideration. In such event, it is necessary to get random measures of the current as well as output voltage of the resonant converter. For that the simulation is made on the LLC resonant converter with random measures at the duty cycle of the switches. To implement the ANFIS controller the gathered data were employed. At training phase the adaptive error back propagation technique was utilized again.

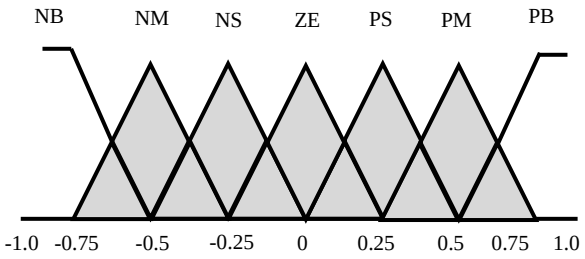

Membership function for error(X)

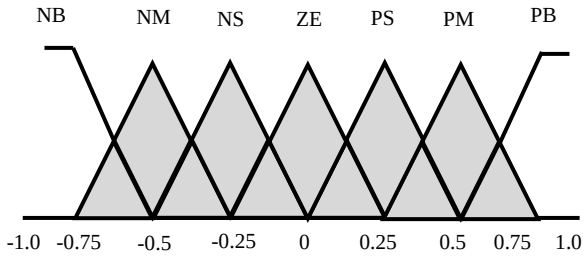

Membership function for Change in error(Y)

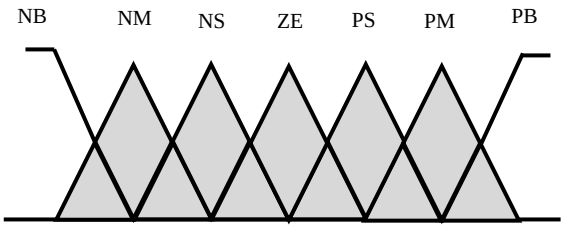

Membership function for Duty cycle (Z)

Fig.11. Membership function of the ANFIS control system

The ANFIS controller proposed in this paper considers X and Y are the input parameters which are error and change in error respectively and Z as the output parameter is the change in duty cycle. In LLC resonant converter the ANFIS control technique is implemented and the implementation results were noted. The summation of the last duty cycle [z(k−1)] and the estimated variation in duty cycle Z produces the duty cycle z(k), in k th sampling time.

$$z(k) = z(k-1) + Z \quad (22)$$

Some of the ANFIS memberships such as NB, NM, NS, Z, PS, PM, PB are given which are expanded as Negative Big, Negative Medium, Negative Small, Zero and Positive Small, Positive Medium, and positive Big respectively.

Development of The ANFIS Controller

To compute the error X and change in error Y signals the instant RMS measures of the sine reference and load voltage at each sampling interval are employed and these X and Y signals are used as the input of the ANFIS controller.

$$X = V_r - V_L \quad (23)$$

$$Y = X - PX \quad (24)$$

Where $V_r$and $V_L$is the reference and actual output voltages respectively. The ANFIS controller decides the duty ratio of the converter. If the output voltage continuously increasing linearly with less current during charging then the ANFIS controller would keep the voltage increase to attain the desired point. In ANFIS controller a small drop at output voltage may increase the entire output voltage of the converter through changing the duty cycle. MATLAB/Simulink software is employed to conduct the closed loop simulation of the LLC resonant converter by employing ANFIS. Based on the error and change in error, the duty cycle measure is evaluated. In MATLAB parameter instructions and function blocks are available that are needed to update the novel duty cycle of the pulse generators.

6. Experimental Results And Analysis

A full bridge LLC resonant dc/dc converter is established that requires a 1.6 kW laboratory prototype. In order to apply the changes in input voltage and load, an additional auxiliary test board is designed in which the load and voltage variations are taken as step functions at exact times.

The Piccolo TMS320F28069 control card [32] is a Texas Instrument that comprises a DSP microcontroller of 32-bit floating point. It is employed to apply control algorithms to control the auxiliary board. For power MOSFET switches, it generates pulse frequency modulation. To implement algorithms such as the PID, Spectator and ANFIS in Digital Signal Processor, the above mentioned control algorithms should be composed on high level C language. This requires a TI's Code Composer Studio (CCS) which may or may not contain the configuration of activated Floating Point Unit (FPU) of F28069 device

In order to run the instruction code from RAM memory, it is necessary to program the produced machine code into on chip RAM memory through CCS. The experimental setup specifying every unit observed here is shown in Fig. 12.

The performance of an ANFIS, PID and Spectator controllers are analyzed for discovering the improved one. Matlab is used to implement the controllers.

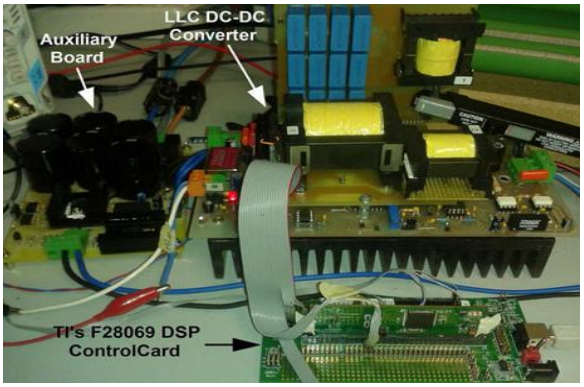

Fig.12. Proto type model of 1.5 kW LLC resonant converter.

A. LLC resonant dc/dc converter: Working principle, open loop transient and frequency responses

In this section, various functionalities of LLC resonant dc/dc converter such as working principle, open loop transient and frequency responses are discussed. Initially, it is necessary to depict ZVS execution of MOSFET switches. For that switching waveforms of LLC resonant tank are computed and demonstrated in Figure. 13.

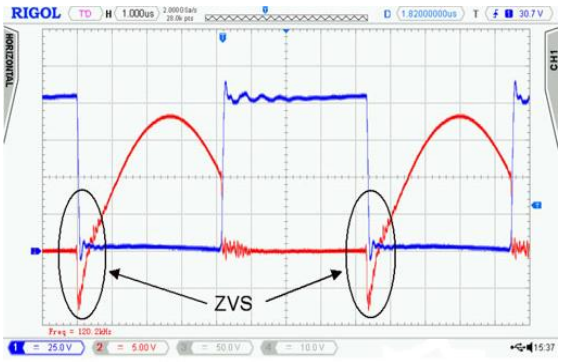

Fig. 13(a). LLC resonant dc/dc converter operation waveforms. Voltage and current waveforms of MOSFET Q_{11} at frequency above f_r (CH1 (square waveform): 25 V/div, CH2: 5 A/div, Time: 1 µs/div).

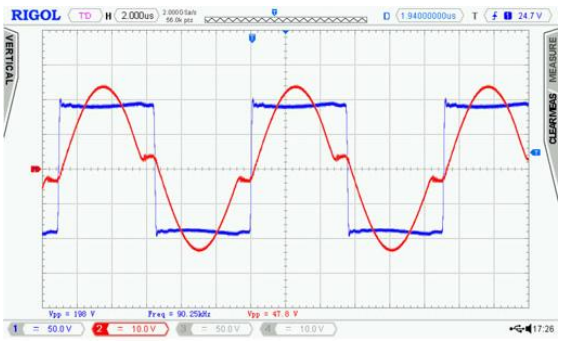

Fig. 13(b) Resonant LLC tank voltage and resonant inductor current at frequency below f_r (CH1 (square waveform): 50 V/div, CH2: 10 A/div, Time: 2 µs/div).

For all experiments, the output power and voltages are set to 1000V and 200V respectively and these experiments were executed without any controller. Fig .13 (a) presents the current and voltage waveforms of Q_{11} MOSFET where the resonant frequency f_r is above than the frequency. Negative current is obtained at the switch on time and it flows through the MOSFET's reverse body diode. At that instant, it preserves their drain source voltage of about 0V.

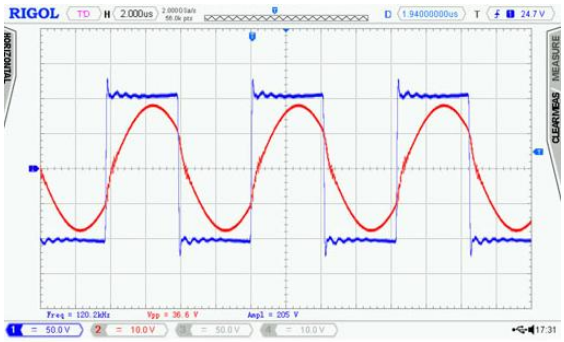

Fig. 13(c) Resonant LLC tank voltage and resonant inductor current at frequency above f_r (CH1 (square waveform): 50 V/div, CH2: 10 A/div, Time: 2 µs/div)

At all power MOSFET switches, the ZVS is turned on through this operation. Fig. 13 (b) and 13(c) shows the voltage and current switching waveforms of resonant LLC tank circuit at lower and higher frequencies than f_r respectively. These figures also demonstrate the ZVS operation of all the switches.

7. Hardware Implementation

Fig. 18 (a), (b) and (c), demonstrates the transitory responses verses PID controller, Spectator controller and ANFIS controller respectively. When the required output voltage is set to 175 V, then the output current is frequently changed from 3A to 6A, and vice versa.

From these figures it can be observed that the rising current edges have 15V, 8V, and 5V output voltage drops; and the falling edges have 8V, 6V, and 5V voltage gain for PID controller, spectator controller, and ANFIS controller respectively.

Moreover, all three controllers respond the output current of rising and falling edges with its settling time such as PID controller has the settling time of 1.2 and 1.5 ms, the spectator controller 0.4ms at both instances and the ANFIS controller has the settling time of 0.35ms. Through this experiment it is clearly show that the proposed PID controller posses better performance when compared to PID and spectator controllers.

Fig. 18. (a). Transitory response of the resonant converter versus step changes in output load by: (PID controller,)

Fig. 18. (b). Transitory response of the resonant converter versus step changes in output load by: (Spectator controller.

Fig. 18.(c). Transitory response of the resonant converter versus step changes in output load by: (Proposed ANFIS controller)

As exposed in those figures, the output voltage changes regarding the input voltage conflict are almost 25V, 14V and 10V for PID, Spectator and ANFIS controllers, correspondingly. Furthermore, the output voltage attain its stable state value in rising limit is 2ms and falling limit is 3ms with PID controller, such time is only 0.9 ms for the spectator controller and 0.7ms for the ANFIS controller It is clear from investigational results that the proposed ANFIS controller posses improved transitory response when compared to the spectator and tuned PID controllers. To evaluate the bandwidth of the proposed ANFIS controller technique, a bode diagram is required which has closed-loop system for ANFIS controller, spectator and PID controllers that are educed through simulation and the result is presented in Fig.20.

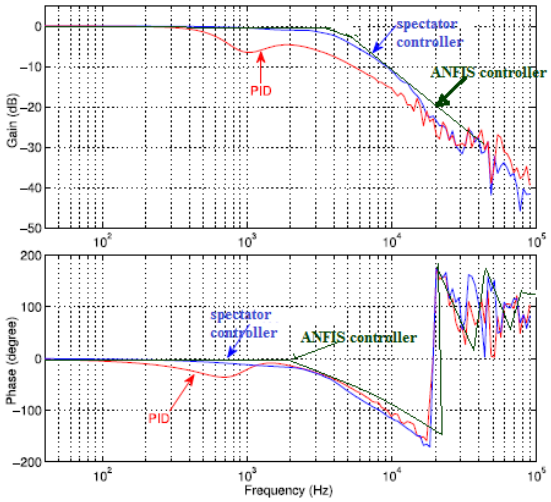

Fig. 19.The bode diagram of the LLC, dc to dc resonant converter closed loop system of ANFIS, Speactator and PID controllers.

ANFIS controller shows that, the bandwidth is considerably enlarged regarding to the Spectator, PID controllers. In general, wider bandwidth represents to smaller rise time. In fact, small transient is expressed obviously through experiments for the technique demonstrated here, regarding to the spectator and PID method.

The performance (in terms of efficiency) of the resonant converter against the output power is shown in Fig. 20. The ANFIS controlled proposed converter posses better performance in extensive limit of output power mainly in smaller output power stages. The output power of the converter was varied from 200 W to 1000W and output voltage set at 200 Voltage. With respect to this change the switching frequency is varied from 124 kHz to 105 kHz. The converter has the switching frequency between 95–175 kHz intervals and the switching frequency of the converter is bounded within 95–175 kHz interval. The higher frequency is adjust to protect gate drivers and MOSFETs from failure and the lower frequency is adjust to assure the operation of ZVS,

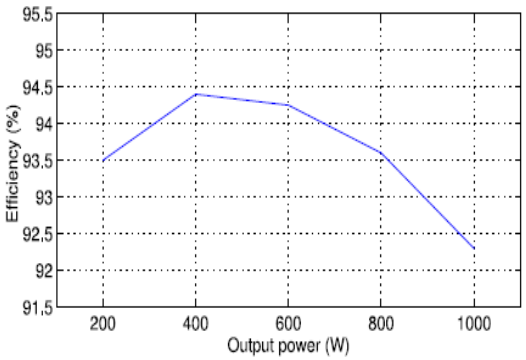

Fig 20.Efficiency versus output power of proposed converter

As shown in Fig. 18 and Fig. 19, the momentary reactions of the ANFIS controller were enhanced in contrast with the spectator and PID controllers. Thus, energy absorption through the converter is much lower with the ANFIS controller throughout transients, by this way better efficiency is achieved. In this paper, our main aim is to design an actual controller instead of efficiency optimization. However, the incurred measures can be enhanced with more exact recognition to attain maximum efficiency. To decrease the switching and transmission losses, the power switches are connected in a parallel manner and/or employing rapid and lesser drain source along with MOSFETs resistance.

IX. CONCLUSION

The presented manuscript describes hypothetical and realistic effects regarding the dynamic investigation and to design controllers of the LLC resonant DC-to-DC converter working under tremendous input circuit voltage and load changes. Subsequently the switching frequency is in the vicinity of the resonant frequency. An exact design has produced in this paper by employing the describing function scheme that aggregates frequency and time domains investigation and derives the representation by separating modulated waveforms into sine as well as cosine waveforms. Elaborated design operations to attain such an estimate model have demonstrated and analyzed. ANFIS controller, Spectator controller and PID controllers are designed. The investigational results proved that the ANFIS controller is much efficient in stabilizing the output voltage under several conditions of input voltage and load. The dynamic reactions under unexpected variations of input and output are compared with the spectator and PID controllers. Investigational analyses showed the quality of the ANFIS controller throughout Spectator and PID controllers.

REFERENCE

[1]http://www.irf.com/product/DC-DC Converters-Integrated POLConverters/

[2] C. Buccella, C. Cecati, and H. Latafat, "Digital control of power converters—A survey," IEEE Trans. Ind. Inform., vol. 8, no. 3, pp. 437–447, Aug. 2012

[3] P. Maftavelli, L. Rossetto,G. Spiazzi, and P. Tenti, "General-purpose fuzzy controller for DC–DC converters," IEEE Trans. Power Electron, vol. 12, no. 1, pp. 79–86, Jan. 1997.

[4] A. Balestrino, A. Landi, and L. Sani, "CUK converter global control via fuzzy logic and scaling factor," IEEE Trans. Ind. Appl., vol. 38, no. 2, pp. 406–413, Mar./Apr. 2002.

[5] E. Vidal, L. Martine, F. Guinjoan, J. Calvente, and S. Gomariz, "Sliding and fuzzy control of a boost converter using an 8-bit microcontroller," Proc. Inst. Elect. Eng., Electr. Power Appl., vol. 151, no. 1, pp. 5–11, Jan. 2004.

[6] M. Qiu, P. K. Jain, and H. Zhang, "An APWM resonant inverter topology for high frequency AC power distribution systems," IEEE Trans. Power Electron., vol. 19, no. 1, pp. 121–129, Jan. 2004.

[7] D. Tschirhart and P. Jain, "ACLL resonant asymmetrical pulse width modulated converter with improved efficiency," IEEE Trans. Power Electron.,vol. 55, no. 1, pp. 114–122, Jan. 2008.

[8] T. S. Sivakumaran and S. P. Natarajan, "Development of fuzzy control of series-parallel loaded resonant converter-simulation and experimental evaluation," in Proc. India Int. Conf. Power Electron., 2006, pp. 360–366.

[9] M. B. Borage, K. V. Nagesh, M. S. Bhatia, and S. Tiwari, "Characteristics and design of an asymmetrical duty-cycle-controlled LCL-T resonant converter," IEEE Trans. Power Electron., vol. 24, no. 10, pp. 114–122, Oct. 2009.

[10] L. Guo, J. Y. Hung, and R.M. Nelms, "Evaluation of DSP-Based PID and fuzzy controllers for DC–DC converters," IEEE Trans. Ind. Electron., vol. 56, no. 6, pp. 2237–2248, Jun. 2009

[11] R. Beiranvand, B. Rashidian, M. R. Zolghadri, and S. M. H. Alavi, "Optimizing the normalized dead-time and maximum switching frequency of a wide-adjustable-range LLC resonant converter," IEEE Trans. Power Electron., vol. 26, no. 2, pp. 462–472, Feb. 2011.

[12] A. G. Yepes, F. D. Freijedo, O. Lopez, and J. Doval-Gandoy, "High-performance digital resonant controllers implemented with two integrators," IEEE Trans. Power Electron., vol. 26, no. 2, pp. 563–576, Feb. 2011.

[13] S. Hong, H. Kim, J. Park,Y. Pu, J. Cheon, D. Han, and K. Lee, "Secondary- Side LLC resonant controller IC with dynamic PWM dimming and dual slope clock generator for LED backlight units," IEEE Trans. Power Electron., vol. 26, no. 11, pp. 3410–3422, Nov. 2011.

[14]. Tomokazu Mishima, Hiroto Mizutani, and Mutsuo Nakaoka, *A Sensitivity-Improved PFM LLC ResonantFull-Bridge DC–DC Converter With LC ntiresonant Circuitry* , IEEE Transactions on power electronics, vol. 32, no. 1, january 2017

[15]. Weimin Zhang,Fred Wang, Daniel J. Costinett, Leon M. Tolbert, and Benjamin J. Blalock, *Investigation of Gallium Nitride Devices in High-Frequency LLC Resonant Converters,* IEEE Transactions on power electronics, vol. 32, no. 1, january 2017